Biochimica et Biophysica Acta 1843 (2014) 1339–1347

Contents lists available at ScienceDirect

Biochimica et Biophysica Acta

journal homepage: www.elsevier.com/locate/bbamcr

Halofuginone improves muscle-cell survival in muscular dystrophies

Anna Bodanovsky [a,1], Noga Guttman [a,1], Hila Barzilai-Tutsch [a], Ola Genin [b], Oshrat Levy [b], Mark Pines [b], Orna Halevy [a,*]

[a] Department of Animal Sciences, The Hebrew University of Jerusalem, Rehovot 76100, Israel
[b] Institute of Animal Science, The Volcani Center, Bet Dagan 52505, Israel

ARTICLE INFO

Article history:
Received 30 August 2013
Received in revised form 25 March 2014
Accepted 26 March 2014
Available online 2 April 2014

Keywords:
Muscular dystrophy
Apoptosis
Satellite cell
Myofibroblast
Myofiber
Halofuginone

ABSTRACT

Halofuginone has been shown to prevent fibrosis *via* the transforming growth factor-β/Smad3 pathway in muscular dystrophies. We hypothesized that halofuginone would reduce apoptosis—the presumed cause of satellite-cell depletion during muscle degradation—in the *mdx* mouse model of Duchenne muscular dystrophy. Six-week-old *mdx* mouse diaphragm exhibited fourfold higher numbers of apoptotic nuclei compared with wild-type mice as determined by a TUNEL assay. Apoptotic nuclei were found in macrophages and in Pax7-expressing cells; some were located in centrally-nucleated regenerating myofibers. Halofuginone treatment of *mdx* mice reduced the apoptotic nuclei number in the diaphragm, together with reduction in Bax and induction in Bcl2 levels in myofibers isolated from these mice. A similar effect was observed when halofuginone was added to cultured myofibers. No apparent effect of halofuginone was observed in wild-type mice. Inhibition of apoptosis or staurosporine-induced apoptosis by halofuginone in *mdx* primary myoblasts and C2 myogenic cell line, respectively, was reflected by less pyknotic/apoptotic cells and reduced Bax expression. This reduction was reversed by a phosphinositide-3-kinase and mitogen-activated protein kinase/extracellular signal-regulated protein kinase inhibitors, suggesting involvement of these pathways in mediating halofuginone's effects on apoptosis. Halofuginone increased apoptosis in α smooth muscle actin- and prolyl 4-hydroxylase β-expressing cells in *mdx* diaphragm and in myofibroblasts, the major source of extracellular matrix. The data suggest an additional mechanism by which halofuginone improves muscle pathology and function in muscular dystrophies.

1. Introduction

Adult skeletal myofibers are terminally differentiated. Therefore, regeneration after injury or in muscular dystrophies (MDs) depends on recruitment of resident satellite cells. Upon appropriate stimulatory signals, satellite cells are activated from the quiescent stage, undergo proliferation and myogenic differentiation, and subsequently fuse with pre-existing myofibers or with other myoblasts, forming myotubes which mature into new myofibers [reviewed in 1,2]. Therefore, the survival and proliferative potential of satellite cells determine the regenerative capacity of skeletal muscles.

Studies have shown that myogenic differentiation is accompanied by apoptosis [3–6]. However, a positive correlation between muscle wasting and apoptotic signals was observed after acute stress, such as electrical stimulation [7] and angiotensin II treatment [8], and in chronic conditions such as myostatin-null mice [9], aging [10], cachexia [11] and MDs [reviewed in 12,13]. In MDs, the muscle wasting due to loss of myofibers is accompanied by fibrosis and muscle-function failure. Necrosis is probably the major leading cause of myofiber degradation in many MDs with sarcolemmal deficiencies, but in the *mdx* mouse model of Duchenne MD (DMD), apoptosis precedes necrosis [12–15]. Apoptotic nuclei were detected in dystrophic muscles, particularly in interstitial cells such as macrophages and activated satellite cells; however, some myofibers with centrally located nuclei were also TUNEL-positive, suggesting DNA fragmentation and apoptosis [15]. Moreover, in the *mdx* mouse model of DMD and in DMD patients, upregulation of pro-apoptotic proteins such as Bax and caspases was observed in myofibers, suggesting that under pathological conditions, these myofibers undergo apoptosis [13,16,17]. Detection of apoptosis and decreased Bcl2 expression have been observed in other MDs such as Limb Girdle MD type 2C patients [18], and congenital MD type 1A [5,19,20].

Halofuginone is a novel anti-fibrotic agent which has been shown to inhibit transforming growth factor β (TGFβ)-dependent fibrosis in various animal models in which fibrosis is the hallmark of the disease [21–23, reviewed in 24]. Recently, halofuginone has been reported to

Abbreviations: CMD, congenital MD; DMD, Duchenne MD; ECM, extracellular matrix; ERK, extracellular signal-regulated protein kinase; DAPI, 4′,6-diamidino-2-phenylindole; MAPK, mitogen-activated protein kinase; MDs, muscular dystrophies; PI3K, phosphoinositide 3 kinase; P4Hβ, prolyl 4 hydroxylase β; αSMA, α smooth muscle actin; TGFβ, transforming growth factor β; YY1, Ying-Yang 1

* Corresponding author at: Dept. of Animal Sciences, The Hebrew University of Jerusalem, P.O. Box 12, Rehovot 76100, Israel. Tel.: +972 8 9489204; fax: +972 8 9489337.
E-mail address: orna.halevy@mail.huji.ac.il (O. Halevy).
[1] Equal contribution.

http://dx.doi.org/10.1016/j.bbamcr.2014.03.025
0167-4889/

inhibit cardiac and skeletal muscle fibrosis and enhance motor coordination and balance in mouse models with early disease onset, such as *mdx* and the laminin α2-deficient dy^{2J}/dy^{2J} mouse model of CMD [25,26], reviewed in [27]. Halofuginone also improved muscle histopathology and function in a dysferlin-knockout mouse model for dysferlinopathy, a late-onset MD [28]. Moreover, halofuginone treatment decreased muscle fibrosis and improved lung and cardiac muscle functions in older *mdx* mice with established fibrosis [29]. In addition to its effect on fibrosis, halofuginone has a direct effect on muscle cells and promotes myotube fusion in primary myoblasts derived from normal and dystrophic muscles [30].

The primary mechanism of halofuginone action is probably inhibition of Smad3 phosphorylation downstream of the TGFβ-signaling pathway, as shown in various cell types [24,31–34], including myoblasts derived from normal and dystrophic muscles [25–27,30]. It has been suggested that halofuginone, *via* inhibiting Smad3 phosphorylation, inhibits the differentiation of fibroblasts into myofibroblasts [24]; the latter possess migratory capabilities and are the primary source for extracellular matrix (ECM) secretion during wound healing and fibrosis [35–37].

It has been reported that halofuginone promotes the phosphorylation of Akt and mitogen-activated protein kinase (MAPK) family members, and enhances the association of Akt and MAPK/extracellular signal-regulated protein kinase (MAPK/ERK) with the non-phosphorylated form of Smad3, resulting in decreased Smad3 phosphorylation [30]. Recently, halofuginone has been reported to reduce inflammation by activating the amino acid starvation response [38].

In this study, we investigated the role of halofuginone in muscle-cell survival of normal and dystrophic mice. We report that halofuginone reduces the number of apoptotic nuclei in the *mdx* mouse diaphragm in general, and that of Pax7-expressing satellite cells and macrophages in particular, together with a reduction in Bax expression in both isolated myofibers and myoblasts, resulting in increased myoblast survival. In addition, halofuginone increases apoptosis in myofibroblasts, the major source of extracellular matrix (ECM) in MD, suggesting an additional muscle-function-enhancing mechanism.

2. Materials and methods

2.1. Reagents

Dulbecco's Modified Eagle's Medium (DMEM), sera and antibiotic–antimycotic solution were purchased from Biological Industries. Collagenase and staurosporine were obtained from Sigma. Ly294002 and UO127 were purchased from Calbiochem. TGFβ was purchased from PeproTech Asia. Halofuginone bromohydrate was obtained from Halo Therapeutics, LLC.

2.2. Mice

C57/BL/6J (Wt) and *mdx* mice were housed in cages under constant photoperiod (12 L:12 D) with free access to food and water. The mice were injected intraperitoneally with either saline or 7.5 μg halofuginone three times a week for 2 weeks, starting at 4 weeks of age. All animal experiments were carried out according to the guidelines of the Volcani Center Institutional Committee for Care and Use of Laboratory Animals (IL-234/10).

2.3. Physiological parameters

Motor coordination and balance were evaluated with an accelerating single-station Rota-Rod treadmill (Med Associates, Inc.) as previously described [25]. In brief, the mice were placed one at a time on the rod, which was rotating at an initial speed of 3.5 rpm; the speed was gradually increased from 3.5 to 35 rpm over a period of 5 min, and the time that the mice stayed on the rod was recorded. The mice were subjected to three successive trials in each session, and the test was repeated on two consecutive days. The performance of each mouse was measured as the mean of its best individual performances over the three trials on the second day.

2.4. Cell preparation

Primary myoblasts and fibroblasts from the diaphragm of *mdx* mice were prepared as described previously [30,39]. Primary cultures and C2 myogenic cell line [40] were grown in DMEM supplemented with 20% (v/v) fetal calf serum. Cells were plated sparsely at 4×10^3 or 5×10^4 cell/cm^2 for C2 muscle cells and primary myoblasts and fibroblasts, respectively, for 1 day, after which the medium was replaced with fresh medium, with or without 10 nM halofuginone. In some cases cells were immunostained for fibroblast-specific protein1 using a monoclonal antibody (Abnova, 1:100).

2.5. Single-myofiber preparation and immunostaining

Single muscle myofibers were isolated from the gastrocnemius muscle of 6-week-old *mdx* and Wt mice, as described [41,42]. Briefly, mice were sacrificed and the gastrocnemius muscles were carefully removed. The outer connective tissue was removed and the muscles were immersed in a 2.5-ml solution of 0.28% (w/v) collagenase type I in DMEM for 60 min for Wt mice or for 90 min for *mdx* mice. The collagenase-treated muscle was then transferred into horse serum (HS)-coated Petri dishes containing 10 ml of DMEM with 10% (v/v) HS (growing medium) for full coverage of the digested fibers, and triturated with a wide-mouth pipette. Myofibers were then washed three times with 10 ml growing medium and placed in 90-mm coated plates. For immunostaining, the myofibers were transferred to 35-mm plates, fixed with 4% paraformaldehyde followed by incubation with Triton X-100 (0.5% v/v in PBS) and blocking with 20% (v/v) goat serum in PBS. The myofibers were incubated with polyclonal anti-Bax (1:150, Santa Cruz Biotechnology) and polyclonal anti-Bcl2 antibodies (1:150, Calbiochem) overnight at 4 °C, followed by incubation with Alexa 594 goat anti-rabbit (1:300, Jackson) secondary antibody for 1 h at room temperature, and nuclei were then stained with 4′,6-diamidino-2-phenylindole (DAPI). The myofibers were visualized under a fluorescence microscope (Olympus) with a DP-11 digital camera (Olympus).

2.6. TUNEL staining

TUNEL staining was performed with the MEBSTAIN Apoptosis Kit Direct (Medical & Biological Laboratories Co.) according to the manufacturer's protocol. This method detects nucleosome-sized DNA fragments by tailing their 3′-OH ends with digoxigenin nucleotides using terminal deoxynucleotidyl transferase (TdT). Paraffin-embedded muscle sections were deparaffinized and rehydrated, then pretreated with 20 μg/ml proteinase K for 20 min at 37 °C. The slides were then incubated with the TdT buffer containing the enzyme and FITC-labeled nucleotides for 1 h to allow the tailing reaction to occur. After washes, the slides were stained with DAPI. In case of double-immunostaining, slides were immunostained with primary monoclonal antibody to β-dystroglycan (1:50; Abcam) or to polyclonal antibodies to either Pax7 (1:100; Abcam), Bax (1:50), α smooth muscle actin (SMA, 1:100; Cell Marque), prolyl-4 hydroxylase ($P_4H\beta$, 1:100; Proteintech Group, Inc.), macrophages (1:200; Acris Antibodies) followed by secondary Alexa 488 donkey anti-mouse or Alexa 594 goat anti-rabbit antibody (1:300; Jackson), prior to the TUNEL staining. Sequential images of the entire diaphragm from five slides from each mouse ($n = 5$) were taken under a fluorescence microscope using DP-11 digital camera. The numbers of all green-fluorescent TUNEL-positive nuclei, DAPI nuclei or double-stained cells were counted using CELL B software (Olympus).

2.7. Confocal microscopy

Microscopic observation and image acquisition were performed with an Olympus IX 81 inverted confocal laser-scanning microscope (Fluoview 500) equipped with a 405-nm diode laser, a 488-nm argon-ion laser, a 543-nm helium–neon laser, and a 60 × 1.0 NA PlanApo water-immersion objective. DAPI was excited at 405 nm and the emission was collected through a BA 430–460 filter; "GREEN" was excited at 488 nm and the emission was collected through a BA 505–525 filter; "RED" was excited at 543 nm and the emission was collected through a BA 560 IF filter. The transmitted-light images were obtained by Nomarski differential interference contrast.

2.8. Western blot analysis

Western blot analysis was performed as described previously [43]. Briefly, equal amounts of protein were resolved by 10% SDS-PAGE and then transferred to nitrocellulose membranes (Bio-Rad Laboratories). After blocking, the membranes were incubated with the following primary polyclonal antibodies: rabbit anti-Bax (1:500), anti-Bcl2 (1:500), and rabbit anti-Ying-Yang 1 antibody (YY1, 1:500, Santa Cruz Biotechnology). The transcriptional repressor protein YY1 was chosen because its gene expression is not altered in the diaphragm of *mdx* mice after halofuginone treatment [44].

2.9. Statistical analysis

The data were subjected to one-way analysis of variance (ANOVA) and to all-pairs Tukey–Kramer HSD test using JMP® software [45].

3. Results

3.1. Halofuginone treatment reduces the number of apoptotic cells in mdx mouse diaphragms

Six-week-old *mdx* mouse diaphragm exhibited fourfold higher numbers of apoptotic cells compared with Wt mice as determined by TUNEL assay (Fig. 1Aa,c and B). Halofuginone treatment of 4-week-old Wt mice for 2 weeks (7.5 μg, three times per week) did not change the percentage of apoptotic cells out of total nuclei in the diaphragm (Fig. 1Aa,b and B). However, halofuginone treatment significantly reduced the percentage of apoptotic cells in the *mdx* mice (over twofold), returning to close to Wt levels (Fig. 1Ac,d and B). The reduction in the number of apoptotic cells coincided with lower collagen levels in the *mdx* diaphragms (data not shown). Analysis of motor coordination and balance with Rota-Rod demonstrated no difference in the performance of the Wt mice treated or untreated with halofuginone (Fig. 1C). The *mdx* mice performed poorly, while the halofuginone-treated *mdx* mice performed significantly better than the untreated mice as well as the Wt mice, in agreement with previous studies [25].

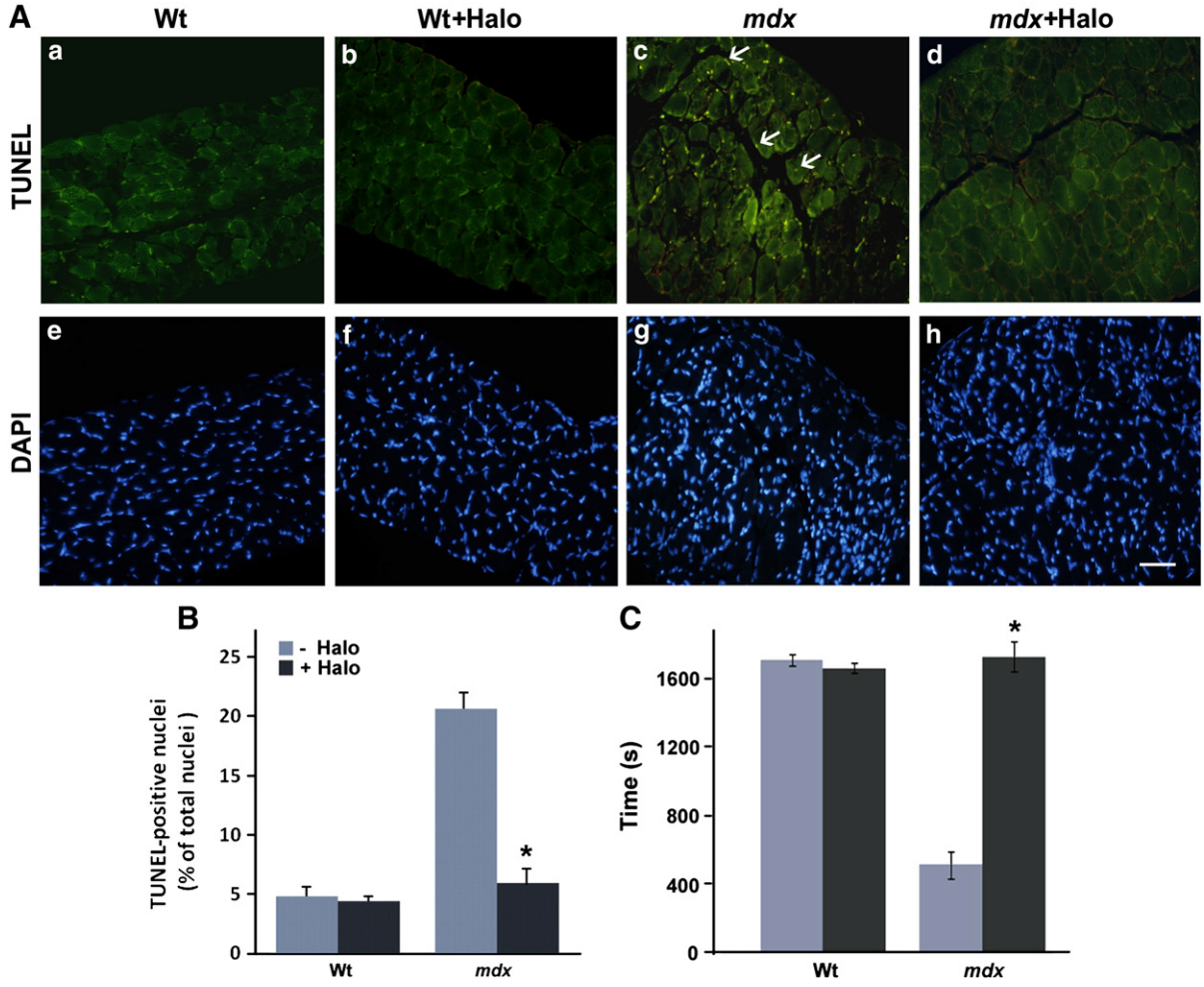

Fig. 1. Halofuginone reduces the number of apoptotic cells in *mdx* muscle. (A) TUNEL staining of diaphragms from Wt (a,b,e,f) and *mdx* (c,d,g,h) mice, with (b,d,f,h) or without (a,c,e,g) halofuginone treatment (Halo; 7.5 μg/mouse, three times a week for 2 weeks, starting at 3 weeks of age). Arrows point to TUNEL-positive nuclei. Bar, 25 μm. (B) Quantitative analysis of TUNEL-positive nuclei presented as percentage of total DAPI-stained nuclei. (C) The effect of halofuginone on motor coordination. A significant enhancement in Rota-Rod performance was observed in the *mdx* mice that were halofuginone-treated (n = 6–8). *Significant difference, within each mouse strain, at $P < 0.05$.

3.2. The location of apoptotic cells in mdx diaphragm

A double-immunostaining of diaphragms derived from 6-week-old *mdx* mice for TUNEL and for Pax7, a marker for satellite cells [1,2], followed by quantitation analysis per total TUNEL-expressing nuclei revealed that the majority of the TUNEL-positive cells were satellite cells (Fig. 2A and E). In some cells, the double-labeling of Pax7 and TUNEL did not entirely merge with the partially degraded nucleus (DAPI staining) (Supplement 1). This may be due to the nature of this staining which may result from changes in antigen distribution

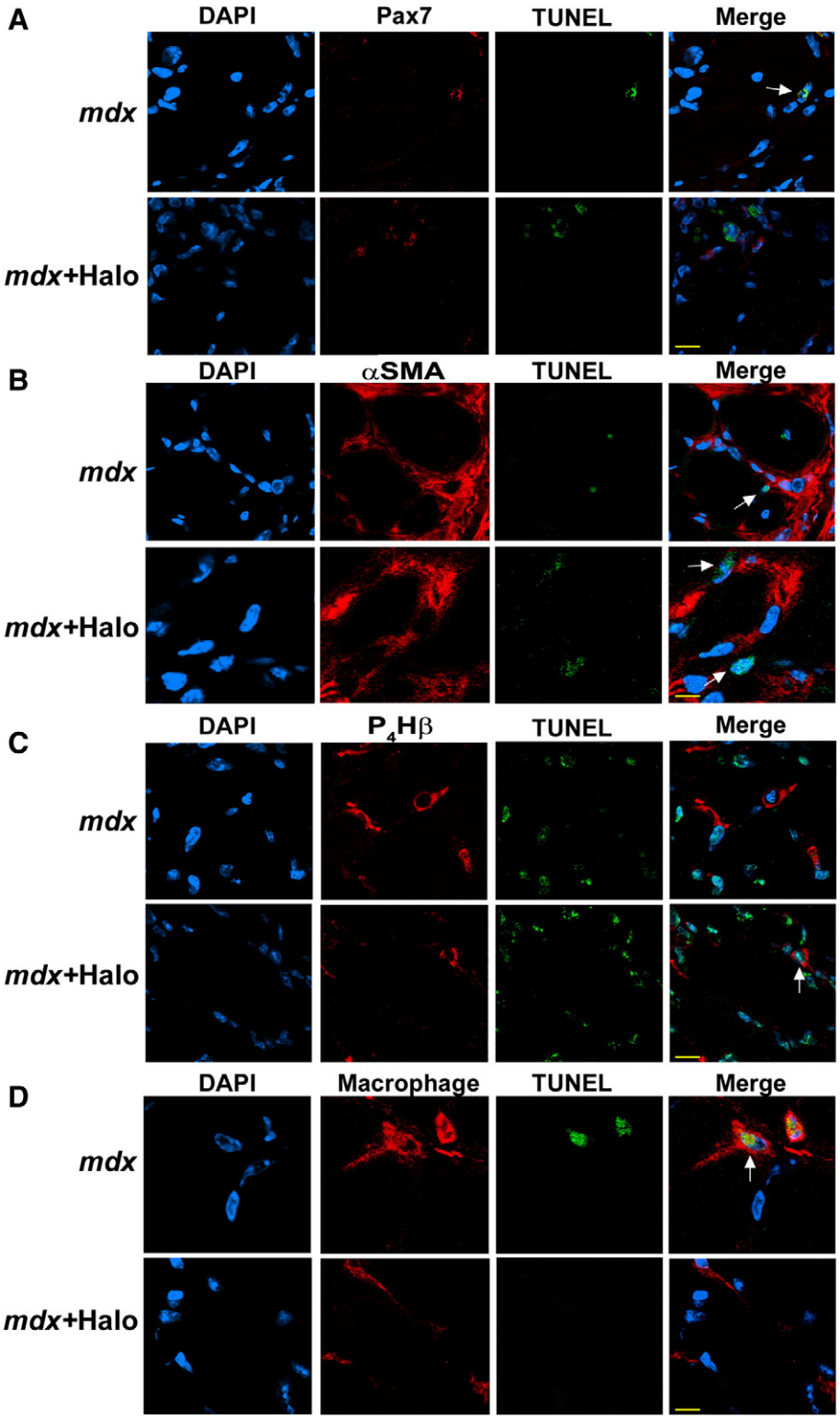

Fig. 2. Localization of apoptotic cells in *mdx* mouse diaphragm and the effect of halofuginone. Double-immunostaining for TUNEL and Pax7 (A), αSMA (B), $P_4H\beta$ (C) and macrophages (D) of diaphragm sections derived from 6-week-old *mdx* mice. White arrows point to TUNEL-positive nuclei. Bar, 10 μM in A, B (*mdx* + Halo), C and D; 20 μM in B (*mdx*). (E) Quantitation analysis of cells positive for both, TUNEL and either Pax7, αSMA, $P_4H\beta$ or macrophages presented as ratio of total TUNEL-positive cells. (F) Motor coordination or balance on the Rota-Rod was observed between the groups at seven weeks of age (four weeks of treatment). *Significant difference, within each protein (E) or group (F) ($P < 0.05$).

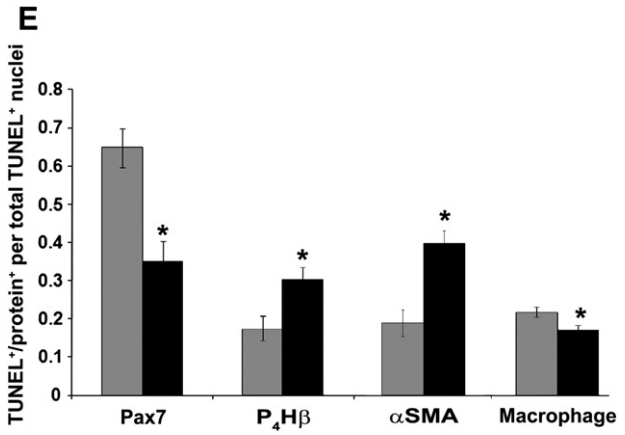

Fig. 2 (*continued*).

associated with nuclear fragmentation. Interstitial cells were also positive for TUNEL, either for macrophages (Fig. 2D) and to a lesser extent for α-SMA (Fig. 2B), and $P_4H\beta$, a collagen cross-linking enzyme (Fig. 2C), both proteins are highly expressed in myofibroblasts [36,37,44]; the latter cells exhibited approximately 15 to 20% of the total TUNEL-positive cells (Fig. 2E). Halofuginone treatment of 4-week-old *mdx* mice for 2 weeks significantly reduced the number of $TUNEL^+$/$Pax7^+$ cells out of total TUNEL-positive cells by almost twofold (Fig. 2B and E), and that of $TUNEL^+$/$macrophage^+$ cells almost 30% (Fig. 2D and E). Conversely, halofuginone treatment significantly enhanced the number of cells co-expressing TUNEL and αSMA and $P_4H\beta$ out of total $TUNEL^+$ cells by twofold and approximately 55%, respectively (Fig. 2B, C and E).

3.3. Halofuginone enhances the survival of myofibers

In light of the results from the TUNEL assay, we next tested the expression of the pro-apoptotic protein, Bax in diaphragm sections derived for 6-week-old Wt or *mdx* mice treated or untreated with halofuginone. As expected, Bax expression was barely observed in Wt diaphragms (Fig. 3) and was even further reduced by halofuginone. High Bax expression was observed in almost all *mdx* myofibers including the ones with central nuclei (*i.e.*, regenerating myofibers). A double-immunostaining for Bax and β-dystroglycan, expressed at the plasma membrane, revealed that Bax staining was with the myofibers (Fig. 3, inner panel). Halofuginone treatment profoundly reduced the Bax levels almost back to those in the Wt.

The expression of the pro- and anti-apoptotic proteins, Bax and Bcl2, respectively, was evaluated in single myofibers derived from untreated or halofuginone-treated *mdx* or Wt mice. Freshly prepared myofibers from gastrocnemius muscle were immediately fixed and immunostained with antibodies against either Bax or Bcl2, side by side, under similar conditions. The proteins were expressed along the entire myofiber. High levels of Bax protein were observed in myofibers derived from untreated *mdx* mice compared while almost no Bax was observed in the halofuginone-treated mice (Fig. 4Aa,b). Conversely, high levels of Bcl2 were seen in myofibers derived from halofuginone-treated mice, in contrast to the minimal levels of expression in the control myofibers (Fig 4Ac,d). As in the tissue staining, no apparent difference in Bax or Bcl2 levels was observed between myofibers derived from halofuginone-treated and non-treated Wt mice (Fig. 4B).

3.4. Effect of halofuginone on myofiber and myoblast survival in culture

Our findings raised the possibility that halofuginone directly improves the survival of muscle cells in *mdx* mice. To further investigate the protective effect of halofuginone on these cells, myofibers were

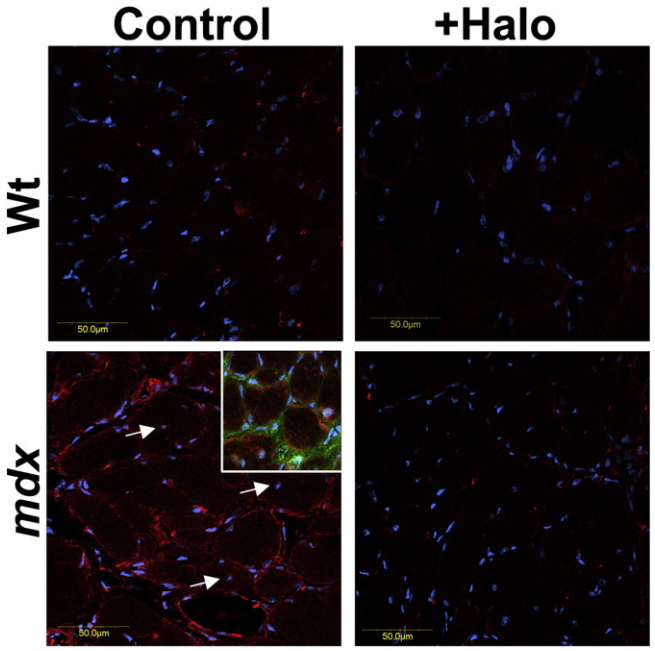

Fig. 3. Pro-apoptotic staining in diaphragms of *mdx* and Wt mice treated or untreated with halofuginone (Halo). Mice were treated as described in Fig. 1 and immunostained for Bax (red). Nuclei were stained with DAPI (blue). Note the high intensity levels of Bax in *mdx* diaphragm section expression across the myofibers, including in centrally-nucleated ones (white arrows), which is diminished by halofuginone, while in Wt mice Bax expression is barely noticed. Inner panel, a double-immunostaining for Bax and β-dystroglycan. Bar 10 μM in inner panel.

prepared from 6-week-old *mdx* mice and immediately incubated in growing medium with or without 10 nM halofuginone for 24 h. The myofibers were fixed and reacted with antibodies against Bax and Bcl2. The non-treated myofibers exhibited high levels of Bax (Fig. 5Aa), whereas the halofuginone-treated myofibers showed markedly decreased levels (Fig. 5Ab). A reciprocal effect was observed with regard to Bcl2; its levels were low in the untreated myofiber and increased in response to halofuginone (Fig. 5Ac,d). No major effect of halofuginone was found on Bax and Bcl2 expression levels in myofibers isolated from Wt mice (data not shown), in agreement with the results shown in Fig. 4B. A western blot analysis for Bax protein in *mdx* myofibers followed by densitometry (normalized to YY1) revealed that halofuginone reduced Bax levels from 0.87 ± 0.25 arbitrary units (AU) in untreated myofibers to 0.48 ± 0.25 AU in treated ones ($n = 4$, $P < 0.05$).

The upregulation of Bax levels found in myofibers derived from *mdx* mice raised the possibility that their associated satellite cells undergo apoptosis, which is reduced by halofuginone. To test this, primary myoblasts were prepared from the gastrocnemius of *mdx* mice and incubated for 24 and 48 h in growing medium with or without halofuginone (replaced daily), and then analyzed for Bax protein levels (Fig. 5B, upper panel). Densitometry analysis revealed that while Bax levels were similar at both time points in the control untreated myoblasts, they were approximately twofold lower in the halofuginone-treated cells (Fig. 5B). Bcl2 protein levels increased after 48 h of halofuginone treatment (Fig. 5B, lower panel).

The effect of halofuginone in preventing apoptosis was observed in *mdx* myoblasts and myogenic C2 cells treated with staurosporine. Cells were plated with or without 10 nM halofuginone for 1 day, after which staurosporine (0.5 μM) was added for an additional 13 h. Cells were then fixed, stained with DAPI and apoptotic/pyknotic nuclei were scored by morphological criteria (Fig. 6A). In both *mdx* myoblasts and myogenic C2 cells treated with staurosporine, numerous nuclei with defragmented DNA (up to 40% of total nuclei) were observed. Treatment of the cells with halofuginone prior to staurosporine addition

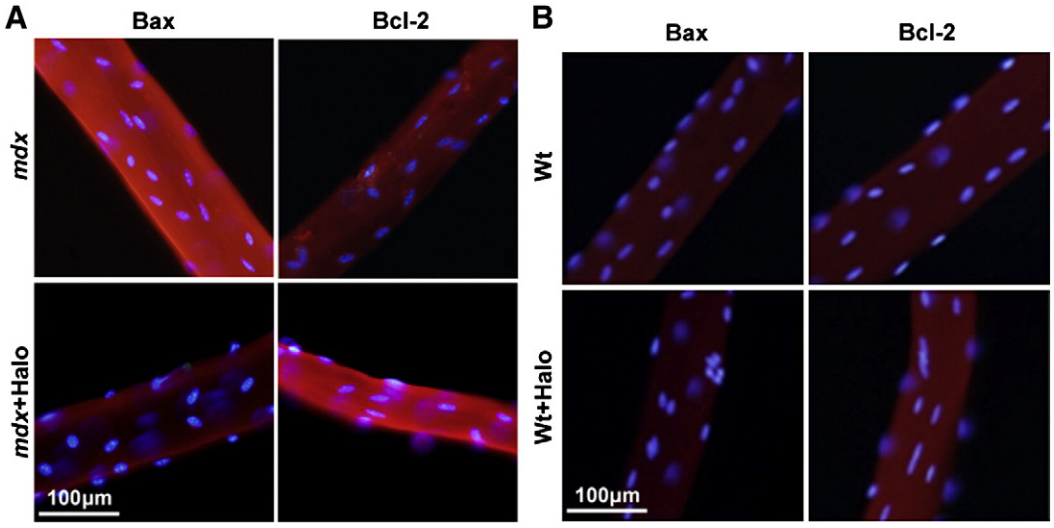

Fig. 4. Pro- and anti-apoptotic protein staining in single myofibers derived from gastrocnemius of untreated and halofuginone-treated (Halo) *mdx* (A) and Wt (B) mice. Single myofibers were immunostained side by side for either Bax (a,b) or Bcl2 (c,d) under similar conditions. Nuclei were stained with DAPI. Note the lower Bax and higher Bcl2 intensity levels in myofibers derived from halofuginone-treated *mdx* mice and the reciprocal results in their untreated counterparts; there was no apparent change in the intensity levels of these two proteins in the treated *vs.* untreated Wt mice.

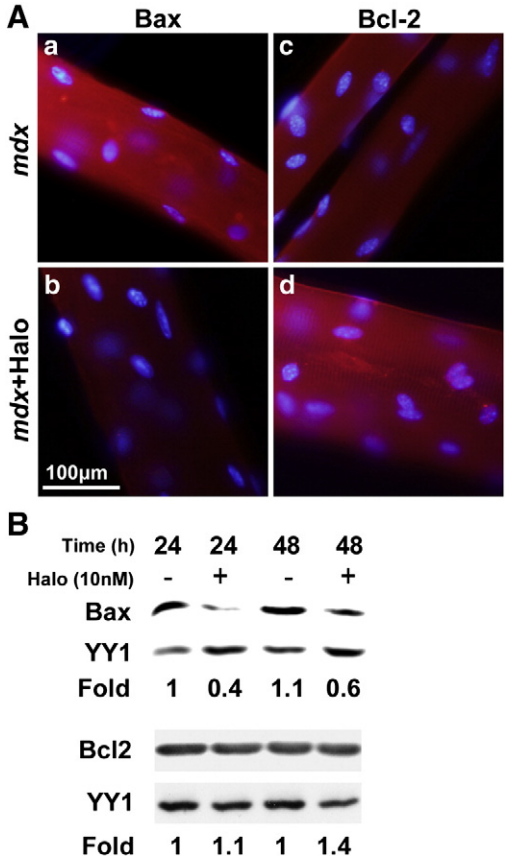

Fig. 5. Direct effect of halofuginone on pro- and anti-apoptotic protein expression *in vitro*. (A) Single myofibers derived from gastrocnemius of 6-week-old *mdx* mice were untreated (a,c) or treated with 10 nM halofuginone (Halo) (b,d) for 24 h, and then stained for Bax (a,b) and Bcl2 (c,d) under the conditions described in Fig. 3. Nuclei were stained with DAPI. (B) Myoblasts derived from *mdx* diaphragms were untreated or treated with halofuginone for 24 and 48 h. Bax and Bcl2 protein levels in cell lysates were analyzed by western blot. Densitometry analysis was normalized to total YY1 and is presented as fold Bax or Bcl2 induction relative to controls at each time point. The results represent one out of three individual experiments.

prevented the staurosporine-induced apoptosis by approximately three- and twofold in the C2 and *mdx* cells, respectively (Fig. 6B). Addition of Ly294002 (25 μM), a stable phosphinositide-3 kinase (PI3K) inhibitor, or UO126 (10 μM), a specific inhibitor for MAPK/ERK signaling pathway, 30 min prior to 24-h incubation with halofuginone to C2 cells reversed the halofuginone effect and increased the percentage of pyknotic nuclei up to 60% and over 70% for Ly294002 and UO126, respectively. In contrast to halofuginone's effect, addition of 10 μM TGFβ for 48 h increased the percentage of pyknotic nuclei out of total nuclei by almost threefold compared to non-treated cells in *mdx* myoblasts (Fig. 6C).

The effect of the combined staurosporine and halofuginone treatment on Bax levels of C2 cells was evaluated (Fig. 6D). Staurosporine addition to C2 cells increased Bax levels more than twofold. Treatment with halofuginone alone had no effect on Bax expression; however, it prevented the staurosporine-induced Bax expression, with levels remaining comparable to those in untreated cells. Similar results were observed for primary *mdx* myoblasts treated with staurosporine (Fig. 6E). Addition of Ly294002 to these cells prior to halofuginone treatment reversed the halofuginone-inhibited effect on Bax levels (Fig. 6F).

Due to its anti-fibrotic properties, the effect of halofuginone on apoptosis of fibroblasts derived from *mdx* muscle was tested. Halofuginone increased the number of pyknotic/apoptotic nuclei threefold (Fig. 7A and B), and immunostaining for a fibroblast-specific marker, fibroblast-specific protein 1, revealed the identity of the pyknotic nuclei as that of fibroblasts (Fig. 7C). Bax protein levels were induced by more than threefold relative to controls (Fig. 7D).

4. Discussion

Apoptosis is one of the main causes of satellite-cell depletion in chronic pathological conditions such as MDs. This study shows that halofuginone, in addition to its capacity to reduce fibrosis and inflammation and improve muscle functions in MDs, is able to enhance the survival of myoblasts and myofibers in dystrophic mice.

In agreement with previous studies [14,46], less than 5% of the total nuclei were apoptotic in the diaphragms of the Wt mice whereas in the *mdx* mice, at as early as 6 weeks of age, a much higher number of apoptotic nuclei was observed. These nuclei were identified as activated satellite cells expressing Pax7—the majority of this cell population was

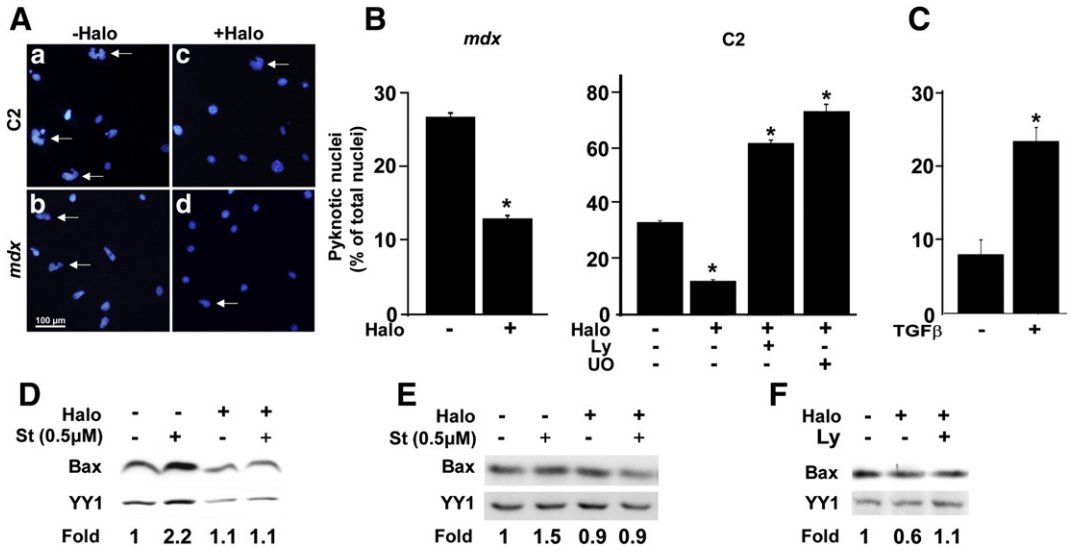

Fig. 6. Reduction of apoptosis by halofuginone in staurosporine-treated muscle cells. (A) C2 muscle cells and primary myoblasts derived from *mdx* diaphragm were plated without (a,c) or with (b,d) halofuginone (10 nM, Halo) for 1 day, after which 0.5 μM staurosporine was added for an additional 13 h. Cells were then fixed and stained with DAPI. Arrows indicate pyknotic/apoptotic nuclei. (B) The apoptotic nuclei were counted and data are presented as percentage of total nuclei. To additional group of C2 cells, Ly294002 (Ly) and UO126 (UO) were added 30 min, prior to halofuginone addition (right panel). (C) *mdx* primary myoblasts were treated with or without TGFβ (1 ng/ml) for 48 h and cells were then fixed and stained with DAPI detected for pyknotic/apoptotic nuclei. Values are expressed as means ± SE of three independent experiments in which more than 2000 cells were examined. *Significantly different at $P < 0.001$ and $P < 0.05$ for B and C, respectively. (D) C2 muscle cells or *mdx* primary myoblasts (E) were treated with or without halofuginone as in A to induce apoptosis and with staurosporine (St) for 6 h. Bax expression levels were analyzed by western blot in cell lysates. (F) *mdx* primary myoblasts were treated with or without halofuginone and with and without 25 μM Ly294002 (Ly) as described in B. Densitometry analysis for levels of Bax was normalized to YY1 and is presented as fold induction relative to control at each time point, representing one out of three individual experiments.

apoptotic (Fig. 2), and interstitial macrophages, as previously shown in *mdx* mice and DMD patients [15,17,47,48]. TUNEL-positive cells were also observed in central-nucleus position in myofibers, consistent with the high Bax levels found in the muscle tissue and in isolated myofibers from these mice (Fig. 3), in agreement with previous studies in *mdx* mice [49] and DMD patients [15], suggesting an apoptotic state of the cells prior to degeneration and necrosis [14,48].

The present study shows for the first time that halofuginone reduces apoptosis in dystrophic mice. This was indicated by a marked reduction in the number of apoptotic Pax7- positive cells (*i.e.*, satellite cells), as well as Bax levels in the diaphragms of halofuginone-treated *mdx* mice, reaching close to those in the Wt. Moreover, single myofibers from the halofuginone-treated *mdx* mice exhibited lower levels of Bax and higher levels of Bcl2 than myofibers derived from non-treated mice (Fig. 4A). These myofibers were immunostained immediately after their preparation and the protein levels likely reflect those *in vivo*, supporting the idea that halofuginone is capable of reducing the apoptotic state of myofibers *in vivo*. This protective effect is not specific to *mdx* mice, as similar results were observed in dysferlin-knockout mice (data not shown). Notably, halofuginone's reducing effect on

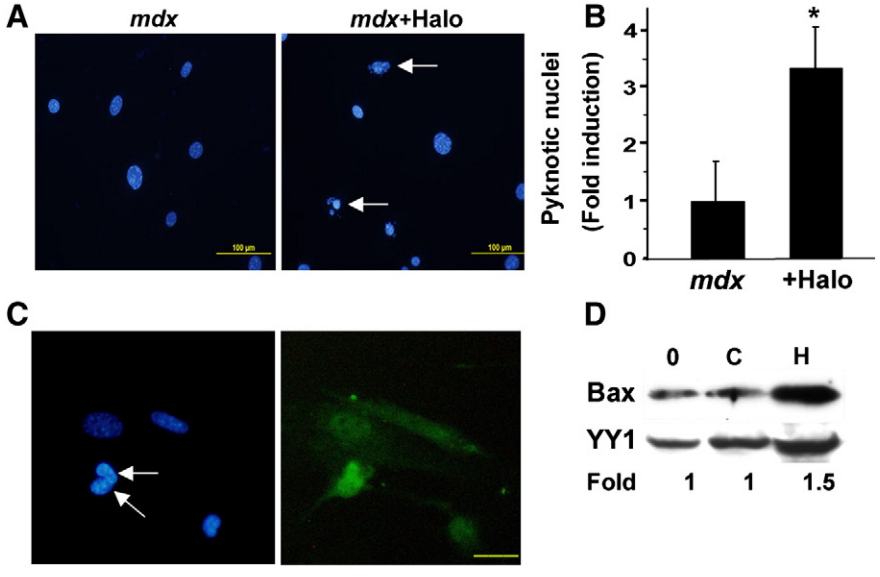

Fig. 7. Halofuginone induces apoptosis in *mdx* fibroblasts. Fibroblasts derived from 6-week-old *mdx* mouse diaphragm were incubated with or without 10 nM halofuginone (Halo) for 24 h, after which cells were DAPI-stained for detection of pyknotic/apoptotic nuclei (A). White arrows point to pyknotic nuclei. Pyknotic cells were quantified and data are means ± SE of three independent experiments in which more than 2000 cells were examined and presented as percent of total nuclei (B). (C) Immunostaining of halofuginone-treated cells for fibroblast-specific protein1 (right panel) and DAPI (left panel), Bar, 50 μM. White arrows point to a pyknotic nuclei. (D) Bax protein expression levels were detected by western blot analysis, normalized to YY1 by densitometry and presented as fold induction relative to controls. 0, time zero; C, control; H, halofuginone.

macrophages was not as profound as on muscle cells. This could be due to the fact that the antibody used to mark the macrophages detects both, M1 inflammatory macrophages and M2, macrophages playing a major role in promoting muscle growth and regeneration; both populations are present in *mdx* mice [50]. As expected, halofuginone did not affect the numbers of apoptotic nuclei or Bax and Bcl2 levels in myofibers of the Wt mice, supporting our basic notion that the major efficacy of halofuginone lies in its ability to improve chronic pathological damage, such as occurs in MDs.

The primary action of halofuginone is suggested to be reduction of fibrosis by attenuating the fibroblast-to-myofibroblast transition, as has been demonstrated in numerous animal models, including MDs [24,27–29]. It is plausible that the beneficial effect of halofuginone on fibroblast survival evolves from its inhibitory effect on fibrosis. However, the data here suggest that halofuginone also has a direct effect on muscle-cell survival. Treatment of *mdx*-derived single myofibers with halofuginone in culture reduced the expression levels of Bax and increased those of Bcl2. The number of pyknotic cells with apoptotic phenotype and the level of Bax expression were lower in halofuginone-treated primary *mdx* myoblasts than in untreated cells. Moreover, a similar inhibitory effect of halofuginone on Bax levels was observed in staurosporine-treated myoblasts, suggesting that at least *in vitro*, halofuginone directly promotes muscle-cell survival.

Recent papers have reported that muscle-derived myofibroblasts from DMD patients show increased resistance to apoptosis [51]. These cells are the main source of muscle collagen, as has been observed in *mdx* [25,52], dy^{2j}/dy^{2j} [26] and dysferlin-knockout mice [28]. In this study, we show that in contrast to its promotive effect on muscle-cell survival, halofuginone treatment of *mdx* mice increases the apoptotic number of the α-SMA and $P_4H\beta$-expressing cells in the diaphragm (Fig. 2) and number of pyknotic nuclei and Bax expression levels in *mdx*-derived fibroblasts (Fig. 7). Interestingly, a similar promotive effect of halofuginone on myofibroblast apoptosis was observed in pancreatic tumors [44]. Taken together, the data suggest that halofuginone protects muscle cells while decreasing the number of myofibroblasts by inducing their apoptotic death; this implies a dual role for halofuginone in this process, which is cell-type specific in muscle. These effects, along with halofuginone's inhibitory effect on the fibroblast-to-myofibroblast transition and subsequent fibrosis, may provide an additional explanation for the promotive effect of halofuginone on cardiac and skeletal muscle functions in various MDs [25,26,28,29].

What mechanism(s) governs the opposite effects of halofuginone on muscle cells and fibroblasts with regard to apoptosis in dystrophic mice? One mechanism might be inhibition of Smad3 phosphorylation downstream of TGFβ, which has been shown to be halofuginone's canonical mode of action in both fibroblasts and myoblasts [24,28,30,33,34]. TGFβ is the major activator of quiescent fibroblasts into differentiated myofibroblasts with migratory and ECM-production properties [53–55]. In contrast, TGFβ has been demonstrated to inhibit myoblast proliferation and differentiation [56–58], at least in part, *via* the Smad3 pathway [59], and to induce apoptosis *in vitro*, as found in this and other studies [60]. In light of these reports and our findings, it is highly likely that the opposite effects of halofuginone on myoblast and fibroblast apoptosis are mediated by the same signaling pathway—the Smad3 pathway downstream of TGFβ.

Halofuginone may also protect muscle cells *via* induction of Akt phosphorylation. Akt is considered a survival factor in many cell types [61,62], including skeletal muscle cells [63], *via* its inhibition of pro-apoptotic signals such as Bad [64] and members of the FoxO family [65], or activation of anti-apoptotic proteins such as Bcl2 [66]. In *mdx* mice, Akt signaling attenuated myofiber degradation, promoted myofiber regeneration and improved muscle function [67]. Attenuation of halofuginone's effect on the number of pyknotic nuclei and Bax expression in myoblasts by the PI3K/Akt signaling pathway inhibitor Ly294002 suggests the involvement of this pathway in mediating halofuginone-induced decrease of apoptosis. Protection of staurosporine-induced apoptosis *via* activation of the PI3K/Akt signaling pathway was observed in cardiomyocytes [68], which may explain in part the increase in cardiac function in *mdx* mice after halofuginone treatment [25,29].

The inhibitory effect of halofuginone on Smad3 phosphorylation in myoblasts [25,30] has been reported to be mediated, at least in part, by phosphorylation of Akt and MAPK/ERK and their association with the unphosphorylated form of Smad3 [30]. Halofuginone's survival effect on myoblasts was reversed by the MAPK/ERK signaling pathway inhibitor UO126. MAPK/ERK pathway was reported to promote myoblast cell survival by stabilizing the cyclin-dependent kinase inhibitor, p21 and inhibiting caspases 9 pro-activation [69]. Therefore, it may well be that MAPK/ERK and Akt signaling increases muscle-cell survival *via* a direct effect on pro- and anti-apoptotic proteins, or indirectly *via* inhibition of Smad3 signaling, or both.

A link between Akt activation, apoptosis and improvement in muscle functions has been observed in other MDs. Inhibition of apoptosis in laminin-2-null mice increased Akt phosphorylation, decreased inflammation, decreased levels of Bax protein and TUNEL-positive myonuclei, and activated caspase-3, resulting in increased lifespan and delayed onset of hind-limb paralysis [5,19,20]. The halofuginone-induced decrease in apoptosis might provide a partial explanation for the improved muscle histopathology and function observed in laminin-α2-deficient mice dy^{2J}/dy^{2J} mice [26].

In conclusion, our findings demonstrate the enhancing effect of halofuginone on muscle-cell survival on the one hand, and fibroblast apoptosis on the other, suggesting an additional mechanism for halofuginone's improved effect on histopathology and muscle functions in dystrophic mice.

Supplementary data to this article can be found online at http://dx.doi.org/10.1016/j.bbamcr.2014.03.025.

Acknowledgements

We thank Edouard Belauso for his help with the confocal microscopy.

References

[1] C.A. Collins, Satellite cell self-renewal, Curr. Opin. Pharmacol. 6 (2006) 301–306.
[2] Z. Yablonka-Reuveni, The skeletal muscle satellite cell: still young and fascinating at 50, J. Histochem. Cytochem. 59 (2011) 1041–1059.
[3] M. Sandri, U. Carraro, Apoptosis of skeletal muscles during development and disease, Int. J. Biochem. Cell Biol. 31 (1999) 1373–1390.
[4] P. Fernando, J.F. Kelly, K. Balazsi, R.S. Slack, L.A. Megeney, Caspase 3 activity is required for skeletal muscle differentiation, Proc. Natl. Acad. Sci. U. S. A. 99 (2002) 11025–11030.
[5] J.A. Dominov, A.J. Kravetz, M. Ardelt, C.A. Kostek, M.L. Beermann, J.B. Miller, Muscle-specific BCL2 expression ameliorates muscle disease in laminin alpha2-deficient, but not in dystrophin-deficient, mice, Hum. Mol. Genet. 14 (2005) 1029–1040.
[6] H. Hirai, M. Verma, S. Watanabe, C. Tastad, Y. Asakura, A. Asakura, MyoD regulates apoptosis of myoblasts through microRNA-mediated down-regulation of Pax3, J. Cell Biol. 191 (2010) 347–365.
[7] B.S. Guo, K.K. Cheung, S.S. Yeung, B.T. Zhang, E.W. Yeung, Electrical stimulation influences satellite cell proliferation and apoptosis in unloading-induced muscle atrophy in mice, PLoS One 7 (2012) e30348.
[8] B.M. Rezk, T. Yoshida, L. Semprun-Prieto, Y. Higashi, S. Sukhanov, P. Delafontaine, Angiotensin II infusion induces marked diaphragmatic skeletal muscle atrophy, PLoS One 7 (2012) e30276.
[9] I. Chelh, B. Meunier, B. Picard, M.J. Reecy, C. Chevalier, J.F. Hocquette, I. Cassar-Malek, Molecular profiles of Quadriceps muscle in myostatin-null mice reveal PI3K and apoptotic pathways as myostatin targets, BMC Genomics 10 (2009) 196.
[10] S. Fulle, L. Centurione, R. Mancinelli, S. Sancilio, F.A. Manzoli, R. Di Pietro, Stem cell ageing and apoptosis, Curr. Pharm. Des. 18 (2012) 1694–1717.
[11] I. Michael, M.D. Lewis, Apoptosis as a potential mechanism of muscle cachexia in chronic obstructive pulmonary disease, Am. J. Respir. Crit. Care Med. 166 (2002) 434–436.
[12] D.S. Tews, Apoptosis and muscle fibre loss in neuromuscular disorders, Neuromuscul. Disord. 12 (2002) 613–622.
[13] D.S. Tews, Muscle-fiber apoptosis in neuromuscular diseases, Muscle Nerve 32 (2005) 443–458.
[14] J.G. Tidball, D.E. Albrecht, B.E. Lokensgar, M.J. Spencer, Apoptosis precedes necrosis of dystrophin-deficient muscle, J. Cell Sci. 108 (1995) 2197–2204.
[15] M. Sandri, C. Minetti, M. Pedemonte, U. Carraro, Apoptotic myonuclei in human Duchenne muscular dystrophy, Lab. Invest. 78 (1998) 1005–1016.

[16] G.R. Coulton, B. Rogers, P. Strutt, M.J. Skynner, D.J. Watt, In situ localization of single-stranded DNA breaks in nuclei of a subpopulation of cells within regenerating skeletal muscle of the dystrophic mdx mouse, J. Cell Sci. 102 (1992) 653–662.
[17] D.S. Tews, H.H. Goebel, Apoptosis-related proteins in skeletal muscle fibers of spinal muscular atrophy, J. Neuropathol. Exp. Neurol. 56 (1997) 150–156.
[18] I. Hadj Salem, F. Kamoun, N. Louhichi, M. Trigui, C. Triki, F. Fakhfakh, Impact of single-nucleotide polymorphisms at the TP53-binding and responsive promoter region of BCL2 gene in modulating the phenotypic variability of LGMD2C patients, Mol. Biol. Rep. 39 (2012) 7479–7486.
[19] M. Girgenrath, J.A. Dominov, C.A. Kostek, J.B. Miller, Inhibition of apoptosis improves outcome in a model of congenital muscular dystrophy, J. Clin. Invest. 114 (2004) 1635–1639.
[20] M. Girgenrath, M.L. Beermann, V.K. Vishnudas, S. Homma, J.B. Miller, Pathology is alleviated by doxycycline in a laminin-alpha2-null model of congenital muscular dystrophy, Ann. Neurol. 65 (2009) 47–56.
[21] F. Levi-Schaffer, A. Nagler, S. Slavin, V. Knopov, M. Pinesygi, Inhibition of collagen synthesis and changes in skin morphology in murine graft-*versus*-host disease and tight skin mice: effect of halofuginone, J. Invest. Dermatol. 106 (1996) 4–8.
[22] M. Pines, A. Domb, M. Ohana, J. Inbar, O. Genina, R. Alexiev, A. Nagler, Reduction in dermal fibrosis in the tight-skin (Tsk) mouse after local application of halofuginone, Biochem. Pharmacol. 62 (2001) 1221–1227.
[23] M. Pines, Inhibition of TGFβ signaling by halofuginone as a modality for pancreas fibrosis prevention, Pancreas 38 (2009) 427–435.
[24] M. Pines, Targeting TGFβ signaling to inhibit fibroblasts activation as a therapy for fibrosis and cancer, Expert Opin. Drug Discov. 3 (2008) 11–20.
[25] T. Turgeman, K. Huebner, J. Anderson, O. Genin, A. Nagler, O. Halevy, M. Pines, Prevention of muscle fibrosis and improvement in muscle performance in the mdx mouse by halofuginone, Neuromuscul. Disord. 18 (2008) 857–868.
[26] Y. Nevo, O. Halevy, O. Genin, I. Moshe, T. Turgeman, M. Harel, E. Biton, S. Rief, M. Pines, Fibrosis inhibition and muscle characteristics improvement in laminin-α2 deficient mice, Muscle Nerve 42 (2010) 218–229.
[27] O. Halevy, M. Pines, Halofuginone and muscular dystrophy, Histol. Histopathol. 26 (2011) 135–146.
[28] O. Halevy, O. Genin, H. Barzilai-Tutsch, Y. Pima, O. Levi, I. Moshe, M. Pines, Inhibition of muscle fibrosis and improvement of muscle histopathology in dysferlin knockout mice treated with halofuginone, Histol. Histopathol. 28 (2013) 211–226.
[29] K.D. Huebner, D.S. Jassal, O. Halevy, M. Pines, J.E. Anderson, Functional resolution of fibrosis in mdx mouse dystrophic heart and skeletal muscle by halofuginone, Am. J. Physiol. Heart Circ. Physiol. 294 (2008) H1550–H1561.
[30] S. Roffe, Y. Hagai, M. Pines, O. Halevy, Halofuginone inhibits Smad3 phosphorylation via the PI3K/Akt and MAPK/ERK pathways in muscle cells: effect on myotube fusion, Exp. Cell Res. 316 (2010) 1061–1069.
[31] O. Halevy, A. Nagler, F. Levi-Schaffer, O. Genina, M. Pines, Inhibition of collagen type I synthesis by skin fibroblasts of graft versus host disease and scleroderma patients: effect of halofuginone, Biochem. Pharmacol. 52 (1996) 1057–1063.
[32] M. Pines, I. Vlodavsky, A. Nagler, Halofuginone: from veterinary use to human therapy, Drug Dev. Res. 50 (2000) 371–378.
[33] T.L. McGaha, R.G. Phelps, H. Spiera, C. Bona, Halofuginone, an inhibitor of type-collagen synthesis and skin sclerosis, blocks transforming-growth-factor-beta-mediated Smad3 activation in fibroblasts, J. Invest. Dermatol. 118 (2002) 461–470.
[34] S. Xavier, E. Piek, M. Fujii, D. Javelaud, A. Mauviel, K.C. Flanders, A.M. Samuni, A. Felici, M. Reiss, S. Yarkoni, A. Sowers, J.B. Mitchell, A.B. Roberts, A. Russo, Amelioration of radiation-induced fibrosis: inhibition of transforming growth factor-beta signaling by halofuginone, J. Biol. Chem. 279 (2004) 15167–15176.
[35] M.A. Watsky, K.T. Weber, Y. Sun, A. Postlethwaite, New insights into the mechanism of fibroblast to myofibroblast transformation and associated pathologies, Int. Rev. Cell Mol. Biol. 282 (2010) 165–192.
[36] F. Klingberg, B. Hinz, E.S. White, The myofibroblast matrix: implications for tissue repair and fibrosis, J. Pathol. 229 (2013) 298–309.
[37] R. Kramann, D.P. Dirocco, B.D. Humphreys, Understanding the origin, activation and regulation of matrix-producing myofibroblasts for treatment of fibrotic disease, J. Pathol. 231 (2013) 273–289.
[38] M.S. Sundrud, S.B. Koralov, M. Feuerer, D.P. Calado, A.E. Kozhaya, A. Rhule-Smith, R.E. Lefebvre, D. Unutmaz, R. Mazitschek, H. Waldner, M. Whitman, T. Keller, A. Rao, Halofuginone inhibits TH17 cell differentiation by activating the amino acid starvation response, Science 324 (2009) 1334–1338.
[39] N. Ben Dov, G. Shefer, A. Irintchev, A. Wernig, U. Oron, O. Halevy, Low-energy laser irradiation affects satellite cell proliferation and differentiation in vitro, Biochim. Biophys. Acta 1448 (1999) 372–380.
[40] D. Yaffe, O. Saxel, Serial passaging and differentiation of myogenic cells isolated from dystrophic mouse muscle, Nature 270 (1977) 725–727.
[41] J.D. Rosenblatt, A.I. Lunt, D.J. Parry, T.A. Partridge, Culturing satellite cells from living single muscle fiber explants, In Vitro Cell. Dev. Biol. Anim. 3 (1995) 773–779.
[42] C.A. Collins, P.S. Zammit, Isolation and grafting of single muscle fibres, Methods Mol. Biol. 482 (2009) 319–330.
[43] O. Halevy, Y. Piestun, M. Allouh, B. Rosser, Y. Rinkevitch, R.I. Rozenboim, M. Wleklinski-Lee, Z. Yablonka-Reuveni, The pattern of Pax7 expression during myogenesis in the posthatch chicken establishes a model for satellite cell differentiation and renewal, Dev. Dyn. 231 (2004) 489–502.
[44] I. Spector, Y. Zilbstein, A. Lavi, O. Genin, M. Pines, Involvement of host stroma cells and tissue fibrosis in pancreatic tumor development in transgenic mice, PLoS One 7 (2012) e41833.
[45] J.M.P. SAS, Statistics and Graphic Guide, Version 4, SAS Institute Incorporation, Cary, NC, 2002.
[46] Y. Nakae, P.J. Stoward, M. Shono, T. Matsuzaki, Most apoptotic cells in mdx diaphragm muscle contain accumulated lipofuscin, Histochem. Cell Biol. 115 (2001) 205–214.
[47] O. Danielsson, C. Nilsson, B. Lindvall, J. Ernerudh, Expression of apoptosis related proteins in normal and diseased muscle: a possible role for Bcl-2 in protection of striated muscle, Neuromuscul. Disord. 19 (2009) 412–417.
[48] M. Sandri, A.H. El Meslemani, C. Sandri, P. Schjerling, K. Vissing, J.L. Andersen, K. Rossini, U. Carraro, C. Angelini, Caspase 3 expression correlates with skeletal muscle apoptosis in Duchenne and facioscapulo human muscular dystrophy. A potential target for pharmacological treatment? J. Neuropathol. Exp. Neurol. 60 (2001) 302–312.
[49] Y. Iwata, Y. Katanosaka, Y. Arai, M. Shigekawa, S. Wakabayashi, Dominant-negative inhibition of Ca2+ influx via TRPV2 ameliorates muscular dystrophy in animal models, Hum. Mol. Genet. 18 (2009) 824–834.
[50] J.G. Tidball, S.A. Villalta, Regulatory interactions between muscle and the immune system during muscle regeneration, Am. J. Physiol. Regul. Integr. Comp. Physiol. 298 (2010) R1173–R1187.
[51] S. Zanotti, S. Gibertini, C. Bragato, R. Mantegazza, L. Morandi, M. Mora, Fibroblasts from the muscles of Duchenne muscular dystrophy patients are resistant to cell detachment apoptosis, Exp. Cell Res. 317 (2011) 2536–2547.
[52] S. Zanotti, S. Gibertini, M. Mora, Altered production of extra-cellular matrix components by muscle-derived Duchenne muscular dystrophy fibroblasts before and after TGF-beta1 treatment, Cell Tissue Res. 339 (2010) 397–410.
[53] Q. Yu, I. Stamenkovic, Cell surface-localized matrix metalloproteinase-9 proteolytically activates TGF-beta and promotes tumor invasion and angiogenesis, Genes Dev. 14 (2000) 163–176.
[54] R.A. Evans, Y.C. Tian, R. Steadman, A.O. Phillips, TGF-beta1-mediated fibroblast–myofibroblast terminal differentiation—the role of Smad proteins, Exp. Cell Res. 282 (2003) 90–100.
[55] A.L. Serrano, C.J. Mann, B. Vidal, E. Ardite, E. Perdiguero, P. Muñoz-Cánoves, Cellular and molecular mechanisms regulating fibrosis in skeletal muscle repair and disease, Curr. Top. Dev. Biol. 96 (2011) 1167–1201.
[56] R.E. Allen, L.K. Boxhorn, Regulation of skeletal muscle satellite cell proliferation and differentiation by transforming growth factor-beta, insulin like growth factor I, and fibroblast growth factor, J. Cell. Physiol. 138 (1989) 311–315.
[57] H.D. Kollias, J.C. McDermott, Transforming growth factor-β and myostatin signaling in skeletal muscle, J. Appl. Physiol. 104 (2008) 579–587.
[58] S. Gardner, D. Alzhanov, P. Knollman, D. Kuninger, P. Rotwein, TGF-β inhibits muscle differentiation by blocking autocrine signaling pathways initiated by IGF-II, Mol. Endocrinol. 25 (2011) 128–137.
[59] S. Zhu, P.J. Goldschmidt-Clermont, C. Dong, Transforming growth factor-beta-induced inhibition of myogenesis is mediated through Smad pathway and is modulated by microtubule dynamic stability, Circ. Res. 94 (2004) 617–625.
[60] X. Li, D.C. McFarland, S. Velleman, Transforming growth factor-β1-induced satellite cell apoptosis in chickens associated with β1 integrin-mediated focal adhesion kinase activation, Poult. Sci. 88 (2009) 1725–1734.
[61] M.M. Hill, B.A. Hemmings, Inhibition of protein kinase B/Akt. Implications for cancer therapy, Pharmacol. Ther. 93 (2002) 243–251.
[62] A. Parcellier, L.A. Tintignac, E. Zhuravleva, B.A. Hemmings, PKB and the mitochondria: AKTing on apoptosis, Cell. Signal. 20 (2008) 21–30.
[63] F. Mourkioti, N. Rosenthal, IGF-1, inflammation and stem cells: interactions during muscle regeneration, Trends Immunol. 26 (2005) 535–542.
[64] S.R. Datta, H. Dudek, X. Tao, S. Masters, H. Fu, Y. Gotoh, M.E. Greenberg, Akt phosphorylation of BAD couples survival signals to the cell-intrinsic death machinery, Cell 91 (1997) 231–241.
[65] A. Brunet, A. Bonni, M.J. Zigmond, M.Z. Lin, P. Juo, L.S. Hu, M.J. Anderson, K.C. Arden, J. Blenis, M.E. Greenberg, Akt promotes cell survival by phosphorylating and inhibiting a Forkhead transcription factor, Cell 96 (1999) 857–868.
[66] S. Pugazhenthi, A. Nesterova, C. Sable, K.A. Heidenreich, L.M. Boxer, L.E. Heasley, J.E. Reusch, Akt/protein kinase B up-regulates Bcl-2 expression through cAMP response element-binding protein, J. Biol. Chem. 275 (2000) 10761–10766.
[67] M.H. Kim, D.I. Kay, R.T. Rudra, B.M. Chen, N. Hsu, Y. Izumiya, L. Martinez, M.J. Spencer, K. Walsh, A.D. Grinnell, R.H. Crosbie, Myogenic Akt signaling attenuates muscular degeneration, promotes myofiber regeneration and improves muscle function in dystrophin-deficient mdx mice, Hum. Mol. Genet. 20 (2011) 1324–1338.
[68] A.H. Liu, Y.N. Cao, H.T. Liu, W.W. Zhang, Y. Liu, T.W. Shi, G.L. Jia, X.M. Wang, DIDS attenuates staurosporine-induced cardiomyocyte apoptosis by PI3K/Akt signaling pathway: activation of eNOS/NO and inhibition of Bax translocation, Cell. Physiol. Biochem. 22 (2008) 177–186.
[69] O. Ostrovsky, E. Bengal, The mitogen-activated protein kinase cascade promotes myoblast cell survival by stabilizing the cyclin-dependent kinase inhibitor, p21WAF1 protein, J. Biol. Chem. 278 (2003) 21221–21231